ISSN (Print) 1226-1750
ISSN (Online) 2233-6656
Journal of Magnetics 25(4), 534-539 (2020) https://doi.org/10.4283/JMAG.2020.25.4.534

Experimental Observation of Temperature Change Induced by Echo Train Length of Fast-Spin Echo at 3T MRI

Sangwoo Kim[1] and Jae-Dong Rhim[2]*

[1]*Department of Pediatrics, Hanyang University College of Medicine, Seoul 04763, Republic of Korea*
[2]*Department of Radiological Science, Daewon University College, Jecheon 27135, Republic of Korea*

(Received 25 August 2020, Received in final form 23 December 2020, Accepted 23 December 2020)

This study aims to observe and estimate the temperature changes caused by the echo train lengths (ETLs) of fast-spin echo to ensure radiofrequency (RF)-related safety. RF-induced heating on ETL-stepped changes is evaluated using the proton resonance frequency shift (PRF) method and optic-fiber thermography (OFT). The increase in temperature caused by a clinical sequence was compared to that accumulated by the corresponding ETLs. The temperatures are similarly increased in ETLs from 10 to 30 (PRF: 0.109 ± 0.025 °C, OFT: 0.079 ± 0.009 °C), suggesting that a large number of ETLs could be utilized at practical sites. The RF-induced heating in the clinical setting (PRF: 0.775 ± 0.069 °C, OFT: 0.510 ± 0.015 °C) is comparable to the estimated temperature on the ETL-stepped changes (PRF: 0.780 °C, OFT: 0.553 °C). These enable accelerated acquisition with a large number of ETLs to be practically used and RF-induced safety to be thoroughly guaranteed.

Keywords : echo train length, temperature, radio frequency safety, fast-spin echo, magnetic resonance thermography

1. Introduction

Magnetic resonance imaging (MRI) has been far more useful for the detection and prognosis of brain diseases such as multiple sclerosis, various cancers, and degenerative symptoms as compared to methods based on radiation exposure [1-3]. However, its application to humans must comply with the safety guidelines stipulated for the applications of radio-frequency energy (RF) [4]. The United States Food and Drug Administration (FDA) and the International Electrotechnical Commission (IEC) restrict as the level of specific absorption rates (SAR) to a maximum of ~4 W/kg and the temperature increase to within 1 °C [5], but it is difficult to correctly measure RF-induced temperature increase in human bodies as heating is mitigated by the blood perfusion rates associated with the geometry of blood vessels and capillaries [6]. The excess absorption of the RF energy beyond its safety standard causes either local hyperthermic tissues or thermoregulatory imbalance, leading to damages such as burning and apoptosis [4, 5]. Earlier temperature studies have been executed through both the experimental phantom and the simulation, which demonstrate the temperature distribution scaled slightly upstream in comparison to the *in vivo* temperature [7, 8]. Hence, in the context of RF energy absorption, temperature measurements are required to ensure or monitor the safety of subjects during MRI.

The application of fast-spin echo (FSE) causes a reasonable scan time in the clinical setting, leading to the prevention of motion-related artifacts. The accelerated performance depends on the number of echo train lengths (ETLs), that is, the turbo factors [9, 10]. However, the use of a high factor induces not only image blurring owing to excessive T2*-decay but also an increase in SAR that is proportional to the RF duty cycle, flip angle, and electrical conductivity [5, 8-12]. The rise of the ETLs expands the RF duty cycle according to a pulse repetition frequency up-scaled, which contributes to the SAR increase [13, 14]. Several studies have investigated the means to address the challenges mentioned above. Sarkar *et al.* have demonstrated the reduced SAR level by changing refocusing flip-angles associated with the peak pulse power [15], but the variation of the signal-to-noise ratio still remains controversial. An additional attempt has also been made to decrease the SAR using variable-rate selective excitation (VERSE) techniques that transform the RF pulse and gradient shape [9, 16]. The VERSE method is applied without changing the acquisition time

*Corresponding author: Tel: +82-43-649-3301
Fax: +82-43-649-3691, e-mail: radrhim@daewon.ac.kr

and the imaging signal, but it is complicated to implement at a practical site owing to the modification of pulse sequences. On the other hand, the range of the number of ETLs, from a few to 30, is generally proposed to ensure the validity of the reasonable scan time and image quality [10]. Although these results are readily applicable to the clinical setting, the temperature changes within the range of ETLs have yet to be reported. We hypothesized that owing to the theoretical perspective of the calculation of the SAR [8], the temperature changes induced by a relatively high number of ETLs numbers do not differ for rapid acquisition in the clinical setting. Thus, temperature measurements are required to determine the number of ETLs that are applicable for compliance with the above-mentioned safety guidelines in the clinical environment.

Several methods have been implemented to calculate the temperature changes in MRI; for instance, the proton resonance frequency shift (PRF) method [17, 18]. The PRF method makes it easy to acquire the temperature changes in the practice sites; it also exhibits the experimental accuracy of temperature distributions through numerical simulation and in vivo tests [7, 8]. In this study, we employ the PRF temperature method and present each RF-induced heating on the ETL-stepped changes. We then report a temperature estimation accumulated by the individual RF-heating in comparison with a practical MRI sequence to guarantee the RF-safety. The RF-induced temperature changes are included in the safety guidelines, and the temperature increase for the clinical sequence could sufficiently be anticipated. Finally, we conclude the paper with a short summary of the study and the scope for future work.

2. Methods

2.1. Phantom and temperature experiments

A phantom was created to map the temperature distribution for RF-induced heating. The phantom included agar (7 g/L), NaCl (10 g/L), and $CuSO_4$ (1 g/L) to mimic the human condition (Fig. 1(a)). The materials were dissolved in hot water, allowing the corresponding solution to cool at room temperature and solidify in a plastic case. Prior to beginning the experiment, the phantom was located inside the MRI space overnight to meet the temperature equilibrium [8].

The phantom was scanned using a whole-body 3T MRI scanner (Achieva, Philips, Best, Netherlands) with an eight-channel phased-array head coil. To observe the temperature changes caused by the number of turbo factors, the FSE sequences were established by increasing the ETL with five steps from 5 to 30. The scan parameters were as follows: time to repeat (TR) = 3000 ms, echo time (TE) = 26 ms, flip angle = 90°, field of view (FOV) = 160 × 160, matrix size = 516 × 516, slice thickness = 4 mm, slice number = 20, number of averages = 2, ETL = 5/10/15/20/25/30, and total acquisition time = 858/264/288/216/174/164 s. In addition, three-dimensional (3D) gradient-echo (GRE) was used to reconstruct MR thermography for the PRF. The 3D-GRE was individually placed before and after the FSE sequences (Fig. 1(b)) with the following identical parameters: TR = 100 ms, TE = 10 ms, flip angle = 15°, FOV = 160 × 160, matrix size = 216 × 216, slice thickness = 5 mm, number of averages = 1, total acquisition time = 12 s. Each phase image was then extracted from the 3D-GRE for the MR thermography using the PRF [17, 18]. Moreover, an arbitrary pelvic sequence in terms of the clinical setting was employed to observe the actual temperature increase since not only the sequence consists of all fast spin-echo but also the SAR and the period of heating contribute to the degree of the RF-induced heating [8]. The relation is as follows:

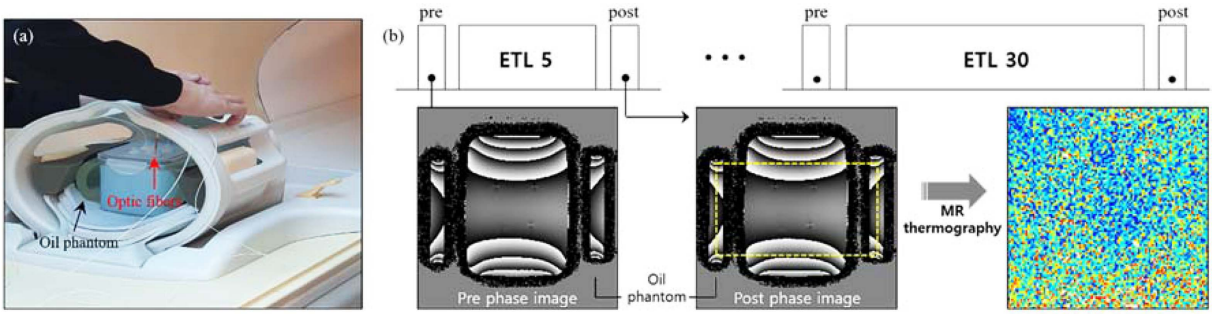

Fig. 1. (Color online) Phantom with agar-gel-mimicked humans and calculation method for MR thermography. (a) Four thermo-optic probes were inserted into center of agar phantom and oil phantoms were placed next to that for temperature correction. (b) Using GRE, phase images acquired before and after ETL applications were reconstructed for MR thermography. Masked region (yellow rectangular dot-lines) was selected to correct RF-induced heating shift caused by oil phantom. ETL = echo train length, MR = magnetic resonance, GRE = gradient echo, RF = radio frequency.

Table 1. SAR values extracted from DICOM format for individual ETL and clinical sequence. SAR are expressed in watt per kilogram (W/kg). ETL = echo train length, SAR = specific absorption rates, COR = coronal plane, AX = axial plane, SAG = sagittal plan, FS = fat saturation, STIR = short time inversion recovery.

ETL	SAR	Pelvic sequence	SAR
5	0.067	T2 COR	0.209
10	0.134	T1 COR	0.183
15	0.140	T2 STIR	0.181
20	0.176	T2 AX	0.208
25	0.212	T2 AX FS	0.193
30	0.218	T1 AX	0.218
		T2 SAG	0.157

$$\mathrm{SAR} = C_{phantom}\frac{\Delta T}{\Delta t}$$

where $C_{phantom}$ is the heat capacity of the phantom (approximately 4200 J/kg/°C) and Δt is the period of heating. Thus, using MATLAB, the corresponding SAR values were extracted from the DICOM files to estimate the temperature increase of the pelvis sequence from the temperature values on the ETL-stepped changes (Table 1). The total number of ETLs for the clinical parameters were 82–16 had a length of 4, 12 had a length of 1, and 3 had a length of 2. Furthermore, the real-time temperatures in each experimental step of the ETL changes and the pelvic sequence were measured through four-optic-fiber (AccuSens; OpSens, Quebec, Canada) thermography (OFT) to compare the pattern of the temperature changes induced by the PRF. Then, averaged temperatures with the standard deviation were calculated by the values through the optic fibers. The whole acquisition process was repeated three times at weekly intervals.

2.2. Reconstruction and quantification of MR thermography

The PRF can be calculated using the phase difference as follows:

$$\Delta T = \frac{\Delta\phi}{\alpha \times \gamma \times B_o \times \mathrm{TE}}$$

where $\Delta\phi$ is the phase difference map calculated using the phase images extracted from before and after a period of FSE, α is the temperature-dependent chemical shift coefficient (-0.01 ppm/K for water), γ is the gyromagnetic ratio, B_o is the strength of the main magnetic field. The temperature maps (ΔT) on each ETL-stepped change and

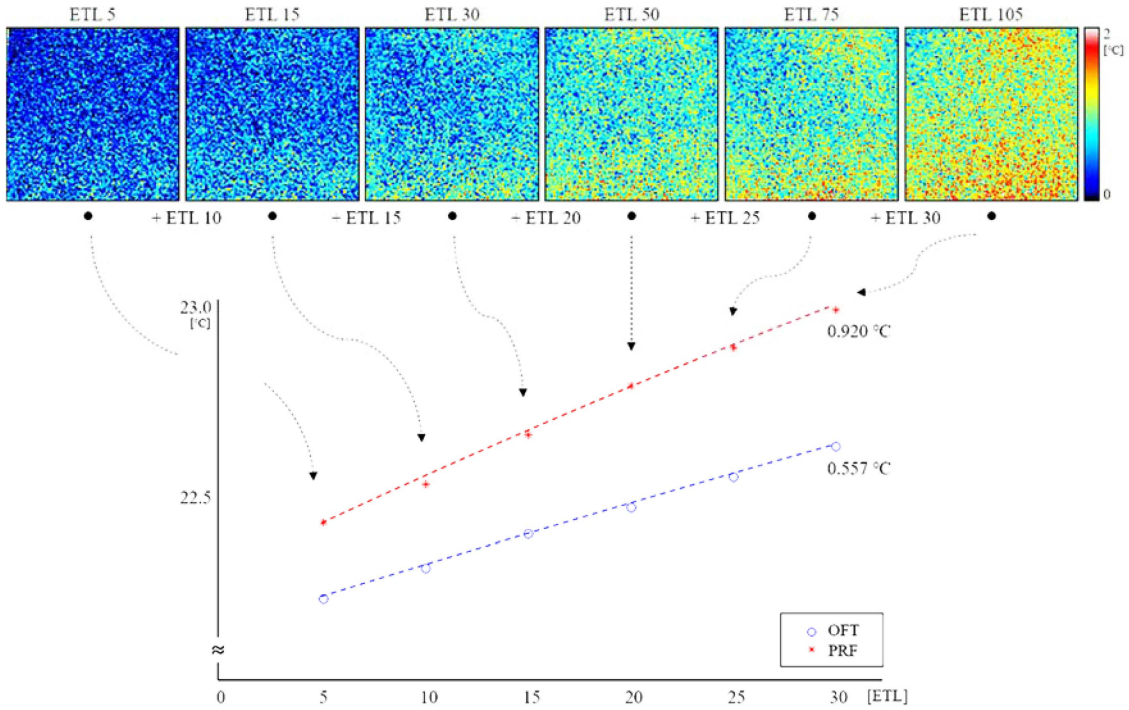

Fig. 2. (Color online) Comparison of PRF-based temperature reconstruction with that of OFT. In PRF, accumulated increases in temperatures according to ETLs are represented with color-coded maps. Both dotted lines (red and blue) are obtained through regression fitting. Note that accumulated temperatures are similarly increased, although PRF values are upscaled. ETL = echo train length, PRF = proton resonance frequency, OFT = optic-fiber thermography.

on the pelvic sequence were reconstructed using this equation above and MATLAB (MathWorks, MA, USA). Rectangular mask regions slightly smaller than the phantom size were selected (within the oil phantom areas; Fig. 1(b)) to quantify the temperature of the PRF. Subsequently, the reconstructed thermal values within the mask regions were determined as the mean and standard deviation and compared to those of the OFT.

3. Results

The temperature changes were measured to determine their impact on the amount number of ETLs. There was an overall increase in the temperature for all the ETLs. Compared to the normal state, the temperature change accumulated by the total ETL, i.e., 105 (the sum of five stepped increases from 5 to 30), was approximately 0.920 °C in the PRF and 0.557 °C in the averaged OFT (Fig. 2). Subsequently, each temperature was differentiated to observe variations in the separate application of the number of ETLs. The lowest number of ETLs, which was the sum of five stepped increases, exhibited a considerable temperature increment (PRF: 0.353 ± 0.024 °C, OFT: 0.160 ± 0.033 °C). Moreover, the average temperatures obtained through successive ETL increments, except the value of ETL 5, increased by approximately 0.109 ± 0.025 °C in the PRF and 0.079 ± 0.009 °C in the OFT (Fig. 3). Although the temperature ranges of the PRFs were greater than those of the OFT, the changed pattern was analogous to the OFT shape scaled by approximately 1.38 times. All the averaged temperatures induced by the number of ETLs are summarized in Table 2.

We also evaluated the temperature changes induced by a pelvic sequence in a clinical setting. The temperatures were increased by approximately 0.775 ± 0.069 °C in the PRF and 0.510 ± 0.015 °C in the OFT, which exhibited an approximately 1.34 times scaled-value, similar to that obtained earlier study [7]. Based on arbitrary values multiplied by the SAR and the heating period of the pelvic examination, temperatures with similar patterns in the ETL-stepped changes were accumulated and compared to those of the actual pelvic experiment. The estimated temperatures were approximately 0.780 °C in the PRF

Table 2. Average temperatures taken for each individual ETL step measured using OFT and PRF methods.

ETL[a]	OFT[b] [°C]	PRF[c] [°C]
5	0.160 ± 0.033	0.353 ± 0.023
10	0.073 ± 0.012	0.108 ± 0.024
15	0.093 ± 0.021	0.121 ± 0.040
20	0.067 ± 0.021	0.131 ± 0.055
25	0.080 ± 0.008	0.108 ± 0.090
30	0.083 ± 0.005	0.100 ± 0.079

[a]ETL = echo train length
[b]OFT = optic-fiber thermography
[c]PRF = proton resonance frequency

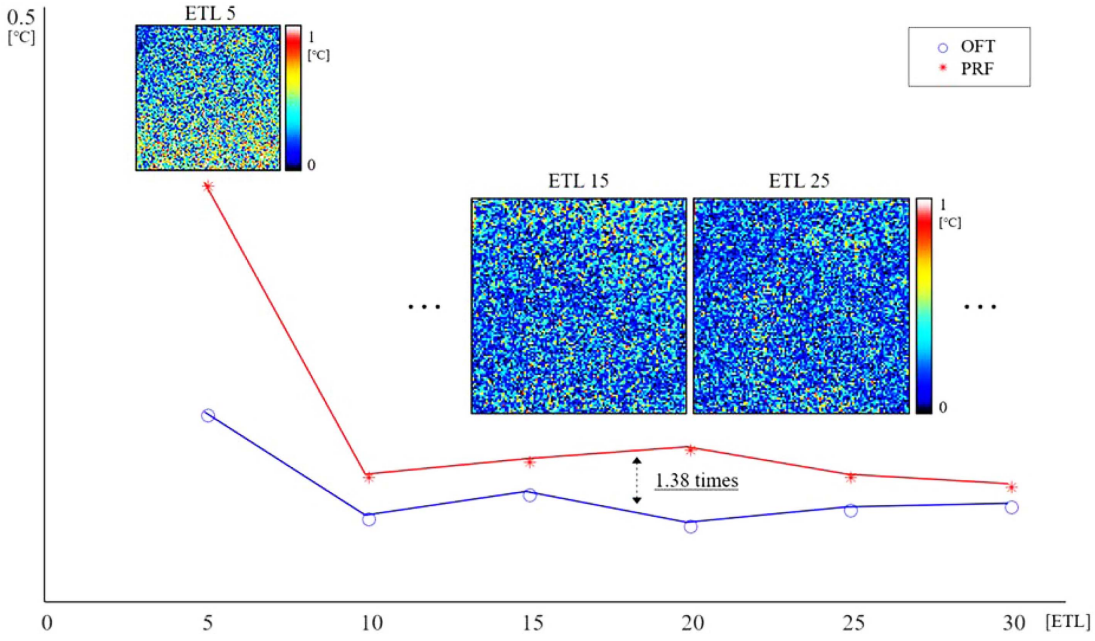

Fig. 3. (Color online) Differential temperature changes with application of ETLs. With exception of ETL 5, RF-induced heating increases similarly (color maps) and PRF is upscaled by 1.38 times compared to OFT. ETL = echo train length, PRF = proton resonance frequency, OFT = optic fiber thermography.

and 0.553 °C in the OFT, which were hardly differentiated from the temperatures increased by the pelvic sequence.

4. Discussion

The objective of this study was to observe and estimate the temperature changes caused by the ETL of the fast-spin echo. The temperature increases were similarly exhibited in the ETL from 10 to 30 (PRF: 0.109 ± 0.025 °C, OFT: 0.079 ± 0.009 °C). In addition, the RF-induced heating by the number of ETLs in the clinical setting–the number 82 (PRF: 0.775 ± 0.069 °C and OFT: 0.510 ± 0.015 °C)–was comparable to accumulating the differential temperature on successive ETLs–a total of 75 (PRF: 0.780 °C and OFT: 0.553 °C). These findings could not only prevent radio-frequency damage such as burning by adjusting their exposure but also accelerate the whole scan time by increasing the number of ETLs.

In clinical and/or research MRI settings, a fast scan time is required to reduce the motion artifacts induced by the subject discomfort and an involuntary condition [9, 10]. The increment in the ETLs in the FSE accelerates image acquisition but is threatened by subject safety because of the increased SAR [9, 19, 20]. We found that the use of ETLs from 10 to 30 illustrated similar RF-induced heating (Fig. 3), suggesting that a large number of ETLs could be utilized for the practical acquisition of T2-weighted images. Earlier studies have demonstrated that the high SAR and the fixed period of heating result in a linear RF-induced temperature increase until the point of the RF shutdown [7, 8], which supports our findings related to elevated temperatures owing to RF absorption. As the RF-induced temperature changes are appreciated through the fact that the SAR are multiplied by the period of heating [8], this theoretical perspective could explain why the long scan time of ETL 5 in this study led to a large increase in temperature. Moreover, similar temperature changes in the other ETLs could be interpreted using the relationship between the increased SAR and the decreased heating period. This means that the accelerated scan time could be realized by the application of the large number of ETLs with a low increase in temperature. That is, ETL 25 would be recommended for practical use, as too high a value of the ETL–above 30–could cause image-blurring due to excessive T2*-decay [11, 12, 20]. However, there was no signal analysis with in vivo conditions such as fat and muscle in this study, which requires additional efforts and will be treated in the future.

We also demonstrated that the temperature changes accumulated by the ETL-stepped change could be estimated during the actual MRI experiment. This result is significant because the RF-induced safety could always be ensured, as suggested by the International Electrotechnical Commission for MRI. The restriction on the SAR is limited to within 2 W/kg in the normal state or 4 W/kg at the first level, which corresponds to a 0.5 or 1 °C increase in the body temperature, respectively [5, 19, 21]. In particular, the RF permission above the first level should be cautiously considered, as the sharp increase in temperature causes biological damages such as burned skin and apoptosis [19, 21, 22]. However, the temperature relies on the visualization of the SAR displayed in the MR scanner. The SAR can be reduced at the clinical site through several approaches. The approaches are long repetition time, small number of total slices or echoes, and an interleaved scan between the high- and low-RF-energy deposits; however, these lead to prolonging the imaging acquisition time [5]. Interestingly, we have presented a means to accelerate the acquisition time using a large number of ETLs through temperature mapping, and the estimated RF-induced heating was almost identical to the actual temperature change for the whole exposure number of ETLs. This indicates that, without the parameter changes, the fast scanning times and the control of thorough RF safety can be simultaneously realized by replanning the total number of ETLs. Consequently, temperature control with short durations for acquisition can reduce RF-induced injuries as well as motion-related artifacts.

Another means to reduce the SAR is to adjust the refocusing flip angle from approximately 60° to 130°. However, this change causes an image contrast or signal-to-noise ratio [5, 9, 23], and, hence, it should be chosen cautiously. In terms of increasing the SAR, as it is proportional to the square of the flip angle [4, 19], a further study is required to determine the changes between the ETL and the refocusing flip angle that contribute to the higher temperature increase. The phantom in this study was also not able to reflect the in vivo condition of the pelvis. This may induce differences in the temperature owing to contributing factors such as material density and heat capacity [4], leading to the requirement of a precise investigation in the future. Finally, a clinical trial should be performed on human subjects to better explain the temperature characteristics in relation to RF safety.

5. Conclusion

We investigated the impact of changes in temperature on the number of turbo factors of fast-spin echo using the proton frequency shift method and optic fibers. We observed temperature increases for individual ETL steps and the corresponding total number that were comparable to a

pelvic sequence of clinical settings. The temperature measurement on the ETL-stepped changes enables accelerated acquisition with a large number of ETLs to be practically used and RF-induced safety to be thoroughly guaranteed. These could also help to prevent motion-related artifacts as well as risks related to radio frequency such as burning.

References

[1] S. Kim, Y. Lee, C.-Y. Jeon, K. Kim, Y. Jeon, Y. B. Jin, S. Oh, and C. Lee, Quant. Imaging Med. Surg. **10**, 789 (2020).
[2] R. Y. Kwong and E. K. Yucel, Circulation. **108**, 104 (2003).
[3] M. A. Schmidt and G. S. Payne, Phys. Med. Biol. **60**, 323 (2015).
[4] C. M. Collins, W. Liu, J. Wang, R. Gruetter, J. T. Vaughan, K. Ugurbil, and M. B. Smith, J. Magn. Reson. Imaging **19**, 650 (2004).
[5] J. Allison and N. Yanasak, Am. J. Roentgenol. **205**, 140 (2015).
[6] P. Bernardi, M. Cavagnaro, S. Pisa, and E. Piuzzi, IEEE T. Bio-med. Eng. **50**, 295 (2003).
[7] S. Oh, Y. C. Ryu, G. Carluccio, C. T. Sica, and C. M. Collins, Magn. Reson. Med. **71**, 1923 (2014).
[8] S. Oh, A. G. Webb, T. Neuberger, B. Park, and C. M. Collins, Magn. Reson. Med. **63**, 218 (2010).
[9] M. A. Bernstein, K. F. King, and X. J. Zhou, Handbook of MRI Pulse Sequences, Elsevier, Cambridge (2004) pp 58-801.
[10] J. P. Mugler, III, J. Magn. Reson. Imaging **39**, 745 (2014).
[11] Q. Qin, Magn. Reson. Imaging **30**, 1134 (2012).
[12] X. Zhou, Z. P. Liang, G. P. Cofer, C. F. Beaulieu, S. A. Suddarth, and G. A. Johnson, J. Magn. Reson. Imaging **3**, 803 (1993).
[13] J. E. Prost, F. W. Wehrli, B. Drayer, J. Froelich, D. Hearshen, and D. Plewes, Magn. Reson. Imaging **6**, 125 (1988).
[14] L. N. Tanenbaum, Magn. Reson. Imaging. Clin. N. Am. **14**, 1 (2006).
[15] S. N. Sarkar, D. C. Alsop, and A. J. Madhuranthakam, R. F. Busse, P. M. Robson, N. M. Rofsky, and D. B. Hackney, Radiology **259**, 550 (2011).
[16] B. A. Hargreaves, C. H. Cunningham, D. G. Nishimura, and S. M. Conolly, Magn. Reson. Med. **52**, 590 (2004).
[17] N. McDannold, Int. J. Hyperthermia. **21**, 533 (2005).
[18] B. Quesson, J. A. de Zwart, and C. T. Moonen, J. Magn. Reson. Imaging **12**, 525 (2000).
[19] L. P. Panych and B. Madore, J. Magn. Reson. Imaging **47**, 28 (2018).
[20] L. Zhang, E. G. Kholmovski, J. Guo, S.-E. K. Choi, G. R. Morrell, and D. L. Parker, Magn. Reson. Imaging **27**, 13 (2009).
[21] L. Zaremba and R. Phillips, Med. Phys. **29**, 1302 (2002).
[22] P. Nordbeck, I. Weiss, P. Ehses, O. Ritter, M. Warmuth, F. Fidler, V. Herold, P. M. Jakob, M. E. Ladd, H. H. Quick, and W. R. Bauer, Magn. Reson. Med. **61**, 570 (2009).
[23] J.-T. A. Chiang, M. Carl, and J. Du, Magn. Reson. Imaging **32**, 259 (2014).